frontiers in Earth Science

ORIGINAL RESEARCH
published: 07 February 2022
doi: 10.3389/feart.2022.818418

Middle Eocene Paleoenvironmental Reconstruction in the Gonjo Basin, Eastern Tibetan Plateau: Evidence From Palynological and Evaporite Records

Licheng Wang[1]*, *Qin Yuan*[2]*, *Lijian Shen*[3] and *Lin Ding*[1]

[1]Key Laboratory of Continental Collision and Plateau Uplift, Institute of Tibetan Plateau Research, Chinese Academy of Sciences, Beijing, China, [2]Key Laboratory of Comprehensive and Highly Efficient Utilization of Salt Lake Resources, Qinghai Institute of Salt Lakes, Chinese Academy of Sciences, Xining, China, [3]MNR Key Laboratory of Metallogeny and Mineral Assessment, Institute of Mineral Resources, Chinese Academy of Geological Sciences, Beijing, China

OPEN ACCESS

Edited by:
Junsheng Nie,
Lanzhou University, China

Reviewed by:
Yunfa Miao,
Northwest Institute of Eco-Environment and Resources (CAS), China
Carina Hoorn,
University of Amsterdam, Netherlands
Bowen Song,
China University of Geosciences, China

***Correspondence:**
Licheng Wang
lichengwang@itpcas.ac.cn
Qin Yuan
yqyq@isl.ac.cn

Specialty section:
This article was submitted to Quaternary Science, Geomorphology and Paleoenvironment, a section of the journal Frontiers in Earth Science

Received: 19 November 2021
Accepted: 11 January 2022
Published: 07 February 2022

Citation:
Wang L, Yuan Q, Shen L and Ding L (2022) Middle Eocene Paleoenvironmental Reconstruction in the Gonjo Basin, Eastern Tibetan Plateau: Evidence From Palynological and Evaporite Records. Front. Earth Sci. 10:818418. doi: 10.3389/feart.2022.818418

The early uplift of the Tibetan Plateau (TP) had a profound influence on the paleoenvironment and paleoclimate. However, we still have little information about the link between the paleoclimatic changes and flora ecosystem caused by the uplift. The Eocene fluvial-lacustrine sequences in the Gonjo Basin, eastern TP, provide excellent archives of the paleoecological and paleoclimatic responses to the surface uplift of the TP. In this study, we investigated a section of the middle Eocene Ranmugou Formation (47.8–>44 Ma) and used the sporomorphs assemblages, sedimentology, and geochemistry of the evaporites to reconstruct the paleoclimate and paleovegetation. The palynological assemblages and coexistence analysis reveal that the middle Eocene ecosystem in the Gonjo Basin was dominated by warm and humid temperate deciduous broad-leaved forests. The $^{87}Sr/^{86}Sr$ ratios (0.709942–0.710062) of all of the gypsum samples are higher than those of contemporaneous seawater, while the $\delta^{34}S$ values (10.3–11.0%) are much lower, indicating a lacustrine environment. Combined with published palynological and paleoelevation data for eastern Tibetan lacustrine basins, we infer that the paleoenvironment changed from warm and humid deciduous broad-leaved forests during 47.8–>44 Ma, to cool and arid temperate forest during 44–40 Ma in the Gonjo Basin, and to arid and cool steppe-desert vegetation in the late Eocene Nangqian Basin. The changes in the paleoclimate and vegetation were primarily driven by the surface uplift of the Central Watershed Mountain, the high topography of which blocked the moisture from the Asian Eocene monsoon.

Keywords: palynology, vegetation, paleoclimate, paleoenvironment, Gonjo Basin, Tibetan plateau

INTRODUCTION

The Eocene was a key period for Asian paleoenvironmental changes (Hoorn et al., 2012) and was characterized by a warmer climate than any other interval in the Cenozoic (Zachos et al., 2001). The highest temperatures were recorded during the Paleocene-Eocene transition (Paleocene-Eocene Thermal Maximum, PETM) (Zachos et al., 2008; Cramwinckel et al., 2018). During the Eocene-

Oligocene transition, the expansion of the polar ice sheets marked a sharp global cooling event in the long-term gradual cooling period after PETM and the climate transformed from a greenhouse to an icehouse (Bohaty and Zachos, 2003; Eldrett et al., 2009). The Middle Eocene Climatic Optimum (MECO) was a very short interval (between ~40.5 Ma and ~40 Ma) of warming during this long-term descent witnessing the Asian tectonic development and monsoon intensification (Fang et al., 2021). The proto-Tibetan Plateau (TP) (Lhasa and Qiangtang terranes) reached an elevation of ~4,000 m (Wang et al., 2008). The Central Watershed Mountain attained a near-present altitude (Xiong et al., 2020). In the middle Eocene, the high topography, retreat of the proto-Paratethys Sea, and global cooling intensified the Asian monsoon (Fang et al., 2021). Nevertheless, how the terrestrial ecosystem and climate changed in response to these Eocene events is still not well constrained. The main obstacle to revealing these responses is the absence of an altitude history with a well-constrained chronology. Moreover, previous studies based on palynological and isotope proxies are regionally limited and were conducted in separate continental basins (e.g., the Xining Basin and the Nangqian Basin, Hoorn et al., 2012; Yuan et al., 2020). Therefore, paleoenvironmental reconstruction, including climate and vegetation, under well-constrained paleoaltimetry in basins on the regional scale is crucial to understanding how the ecosystem responded to the uplift of the TP and global cooling.

The Gonjo Basin, located on the eastern part of the Central Watershed Mountain, hosts a thick, successive Paleocene-Eocene sedimentary record (Studnicki-Gizbert et al., 2008). The accurate age constraints based on magnetostratigraphy and radioactive isotopes (Li et al., 2020; Xiao et al., 2021) of uplift history (Xiong et al., 2020) make the ~2,000 m sedimentary sequences in the Gonjo Basin perfect for conducting Eocene paleoclimatic and paleovegetation reconstruction, although the age of the Ranmugou Formation is still controversial. Palynological studies are a useful tool for constraining the age and reconstructing the vegetation, paleoclimate, and paleoecological evolution of a region (Hoorn et al., 2012; Miao et al., 2016; Tang et al., 2020). The use of sedimentology and isotopic geochemistry to study paleoenvironmental changes is also well-established. In this study, we used palynological, sedimentary, and geochemical records of the middle Eocene Ranmugou Formation to discuss the age of the Ranmugou Formation and reconstruct the paleoenvironmental changes in the Gonjo Basin. Then, we compared the climate and vegetation with other continental basins in the northeastern TP and determined the driving forces of the paleoenvironmental changes.

GEOLOGIC SETTING

The TP is composed of the Qiangtang, Lhasa, and Tethyan Himalaya terranes and several sutures between these continental terranes, including the Jinshajiang suture, Longmuco-Shuanghu suture, Bangong-Nujiang suture, and Yarlung-Zangbo suture (Yin and Harrison, 2000; Metcalfe, 2013) (**Figure 1**). The Qiangtang terrane is further subdivided into the southern and northern Qiangtang terranes (SQT and NQT) by the Longmuco-Shuanghu suture, which is believed to be related to the closure of the Paleo-Tethyan Ocean in the Late Triassic (Zhai et al., 2011; Metcalfe, 2013). A series of Cenozoic strike-slip pull-apart basins were developed in the southeastern margin of the TP, including the Nangqian, Shanglaxiu, Gonjo, Markham, Jianchuan, Lanping, and Simao basins. These basins were commonly infilled by alluvial fan and fluvial coarse clastic rocks interbedded with lacustrine mudstone and marls, and these deposits are thousands of meters thick along the faults and suture zone (Zhang et al., 2007).

The Gonjo Basin is located in the northeastern part of the NQT and is bounded by the Jinshajiang suture to the east and the Bangong-Nujiang suture to the west. The Gonjo Basin is a syn-contraction basin (Studnicki-Gizbert et al., 2008) and is composed of an asymmetric syncline controlled by a thrust system (Li et al., 2020; Xiong et al., 2020). The Cenozoic red beds in the Gonjo Basin are divided into the Gonjo and Ranmugou formations. The Gonjo Formation is conformably overlain by the Ranmugou Formation and is unconformably underlain by Lower and Middle Triassic limestone and volcanic rocks (Tong et al., 2017). The Gonjo Formation consists of eolian sandstones in the lower part and fluvial sandstones and siltstones in the upper part (Xiong et al., 2020). The Ranmugou Formation can stratigraphically be divided into three parts. The lower part is mainly composed of massive gray-purple conglomerates interlayered with sandstones (BGMRT, 1993), indicating a distal alluvial fan or fluvial facies (Xiong et al., 2020). The middle part is mainly reddish-brown sandstones, which have been hypothesized to be deltaic deposits (Tang et al., 2017). The upper part consists of green lacustrine carbonaceous shales, carbonates, red mudstone, and evaporites (Studnicki-Gizbert et al., 2008).

Although several geochronological studies have been recently conducted, the ages of these beds remain controversial (**Figure 2**). The previous geochronology studies of the Gonjo red beds were based on palynology and palm fossils. The palm fossil *Sabalites* sp. was initially assigned an Eocene age (He et al., 1983). A Tibetan regional study suggested a Paleocene to Eocene age based on fossil sporomorphs (BGMRT, 1993). Studnicki-Gizbert et al. (2008) identified limited palynomorphs of *Momipites* sp., *Retitricolporites* sp., Taxodiaceae, and/or Cupressaceae sp., *Inaperturites* sp., *Striatricolpites* sp., *Caryaepollenites*, *Psilamonocolpites* sp., *Psilatricolpites* sp., *Tricolpites* sp., and *Schizosporis* sp. and concluded these to be late Eocene and Oligocene deposits. However, the volcanic rocks in the upper Ranmugou Formation yielded an age of ~43 Ma based on Ar-Ar and U-Pb zircon dating methods (Studnicki-Gizbert et al., 2008; Tang et al., 2017). Recently, Xiong et al. (2020) reported several ages for the volcanic rocks in the upper Ranmugou Formation, ranging from 50 Ma to 40 Ma in northern and southern parts of basin. A magnetostratigraphic study in the central part of the basin revealed that the ages of the continuous sequences of the Gonjo and Ranmugou formations ranged from ~69 Ma to 41.5 Ma, of which the Ranmugou Formation is ~65.2 Ma to 41.5 Ma (Li et al., 2020) (**Figure 2**). Xiao et al. (2021) indicated that the Gonjo and Ranmugou formations are 69 to

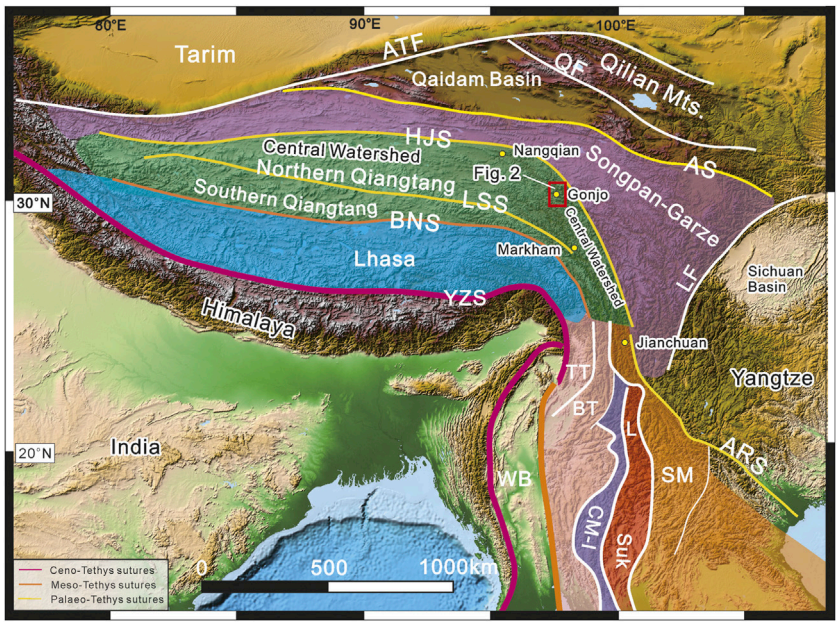

FIGURE 1 | Map showing the main terranes and sutures of the Tibetan Plateau and surrounding areas. ATF: Altyn Tagh fault; QF: North Qaidam fault; AS: Anemaqen suture; HJS, Hoh Xil-Jinshajiang suture; LF: Longmenshan fault; LSS: Longmuco- Shuanghu suture; BNS: Bangong-Nujiang suture; YZS: Yaulung Zangbo suture; ARS: Ailaoshan-Red River suture; TT: Tengchong terrane; BT: Baoshan terrane; WB: West Burma terrane; CM-I: Changning-Menglian-Inthanon suture; L: Lincang Batholith; Suk: Sukhothai Arc terrane; SM: Simao Block.

50 Ma in the central Gonjo Basin, and the Ranmugou Formation was assigned an age ranging between 63.5 Ma and 50 Ma. They believed that the magnetostratigraphic results of Li et al. (2020) were inaccurate due to their isotopic age deriving from other sections. Therefore, the age constraint of the upper Ranmugou Formation lacustrine sequences is still controversial (**Figure 2**). The biostratigraphy based on palynology will be used to limit the age in this study.

MATERIALS AND METHODS

Measured Section and Sedimentology

A 90 m thick section of the upper Ranmugou Formation is exposed in Youzha, Gonjo Basin (30.719468°N, 98.420275°E) (**Figure 3A**). This section is near the core of the Youzha syncline and consists of thin-bedded limestones and marls, siltstones, mudstones, shales, and evaporites (**Figure 3B**). The lower part of the section is characterized by limestones and marls interbedded with thin-bedded gypsum rocks. The middle part of the section is composed of purple siltstones interbedded with shales and mudstones. Ripple marks, parallel bedding, and horizontal bedding are common (**Figure 4**). The lithology of the upper part is mainly dark grey limestones and marls interbedded with thin gypsum rocks and conglomerates. Secondary gypsum usually cuts through the bedding and occurs in veins (**Figure 4**). Based on a previously recovered drill core, the evaporites are composed of gypsum, anhydrite, and rock salts (Chen, 1990). The thickness of the rock salt is up to 356.8 m. It mainly consists of clay gravel and halite, and it exhibits tectonic reworking, salt solution, and leaching. The rock salts that outcrop at the surface are usually conglomerates composed of clay gravels. Due to the Quaternary cover, the thick halite sequences in the core of the syncline are not exposed.

Samples and Analytical Methods

Four gypsum samples were collected for trace element and rare Earth element (REE) analyses and S and Sr isotopic analyses. The trace element and REE contents were obtained via inductively coupled plasma mass spectrometry (ICP-MS) after being treated with 5 M HCl and filtered through a cellulose acetate membrane filter at the Beijing Research Institute of Uranium Geology. For the S isotope analysis, the samples were purified as $BaSO_4$ after combustion with a Eschka reagent, and then, they were treated with V_2O_5 to produce SO_2. The resulting SO_2 was measured using the MAT 251 EM mass spectrometer at the MNR Key Laboratory of Metallogeny and Mineral Assessment, Beijing. The $\delta^{34}S$ values are reported vs. the Canyon Diablo troilite (CDT), and the estimated error is about ±0.2‰. The Sr isotope analyses were performed at the Beijing Research Institute of Uranium Geology. About 10 mg of sample (200 mesh) were dissolved using 4 M HNO_3 after being washed with milli-Q water and dried. The Sr was extracted from the Sr-resin and was analyzed using a Neptune Plus multicollector ICP-MS. The Sr isotopes are reported as $^{87}Sr/^{86}Sr$. $^{87}Sr/^{86}Sr$ values of 0.71022–0.71030 were obtained for standard NBS987. The reported uncertainties of the $^{87}Sr/^{86}Sr$ ratios are 1σ.

A total of 16 limestone and marl samples from the Youzha section were analyzed for the palynological investigations. The sample processing employed a standard technique and was

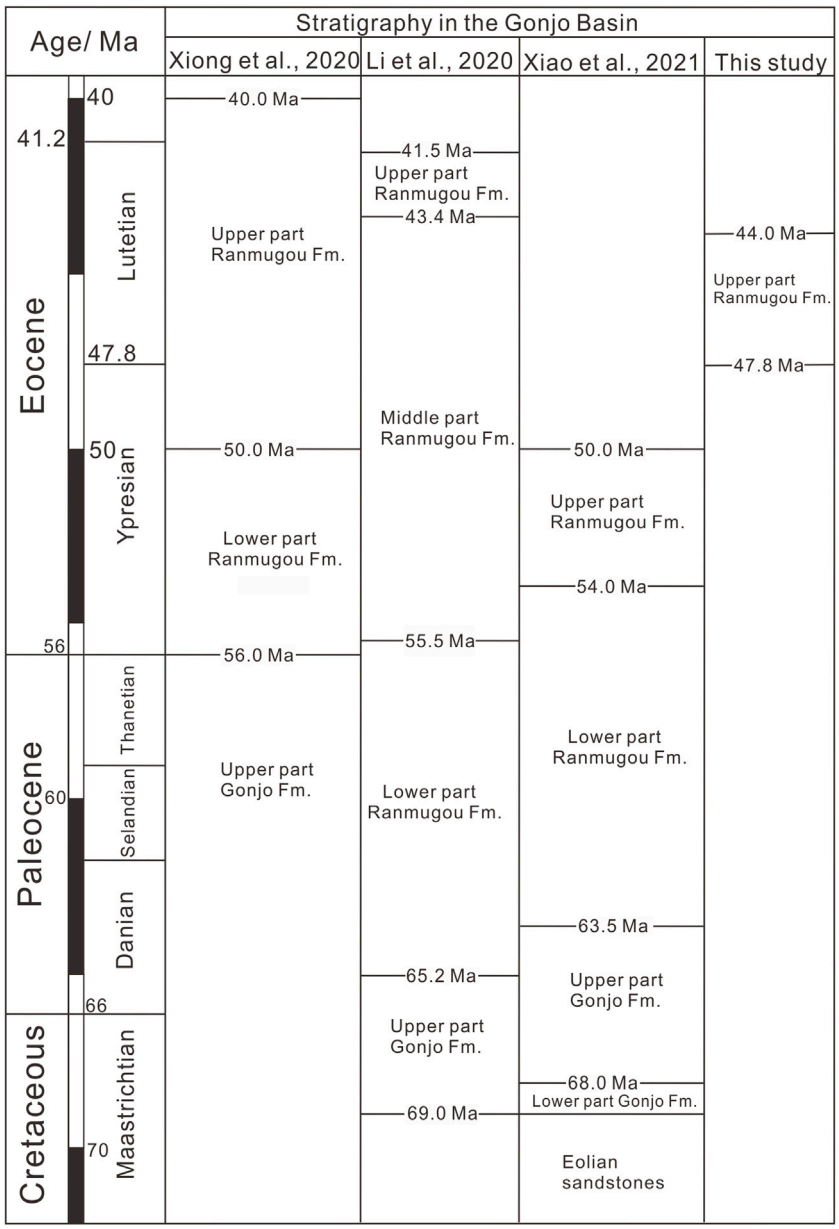

FIGURE 2 | The stratigraphic and geochronological division of the Gonjo Basin.

conducted at the Institute of Geology, Chinese Academy of Geological Sciences. About 50 g of crushed sample (100 mesh) was treated with 15% HCl for 24 h and then washed 3 to 5 times to a neutral pH. Then, the samples were treated with 39% HF for 72 h and were washed to a neutral pH. The residue was sieved through a 10 μm nylon mesh and collected in a 10 ml centrifuge tube (2,500 rpm). The final organic residue was placed in a 1.5 ml centrifuge tube in glycerin jelly and was mounted on microscope slides. The palynomorph identification and photography were performed using a LEICA DM4500P microscope. At least 200 grains from each sample were identified and counted. The coexistence approach (CA) was widely used to quantitatively reconstruct paleoclimate in recent decades (e.g., Quan et al., 2012; Xie et al., 2019), although the CA remains uncertainties (Mosbrugger and Utescher, 1997). The CA is based on assumption that climatic tolerances of a fossil plant are similar to its nearest living relative (NLRs) when its modern affinity is determinable (Quan et al., 2012). We determine NLRs from a Palaeoflora Database (Utescher and Mosbrugger, 1997) and data from Quan et al. (2012) (**Table 2**). We only reconstruct two climatic parameters, i.e., mean annual temperature (MAT) and mean annual precipitation (MAP). It should be noted that the CA was challenged and referred to as "useless" by Grimm and Denk (2012). However, ongoing updates of the database, new successful

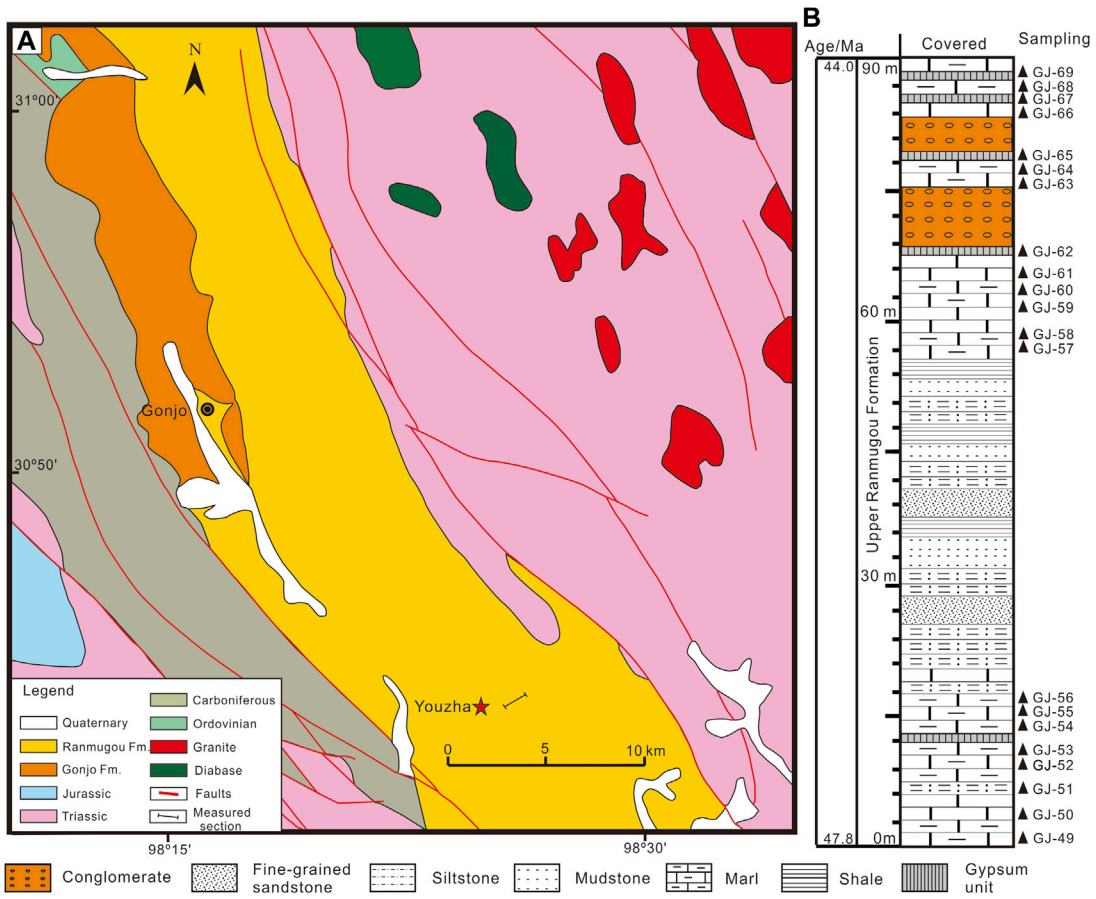

FIGURE 3 | (A) Geological map of the central and southern Gonjo Basin (adapted from Tang et al., 2017). **(B)** The stratigraphic column of the measured section in Youzha, Gonjo Basin. The location is marked with a red star. Geochemical and palynological samples from the upper part of the Ranmugou Formation are marked with black triangles.

tests with modern florals, and probability considerations for a high number of taxa overlapping make the method of paleoclimate reconstructions reliable (Hoorn et al., 2012; Quan et al., 2012; Utescher et al., 2014).

RESULTS

Geochemistry

The most concentrated trace element was strontium (Sr), with concentrations of 96–111 ppm. The V, Co, and Ni contents were much higher (V: 7.9–35.3 ppm; Co: 10.1–10.9 ppm; and Ni: 15.6–18.1 ppm) (**Table 1**), similar to those in the mid-Cretaceous anhydrite in the Mengyejing Formation in the Simao Basin (Xia and Li, 1983). This probably indicates contribution from a deep fluid. The concentrations of other metals such as Sc, Cr, Cu, and Zn range from 0.9 to 7.4 ppm. The REE concentrations are all low and are much lower than the heavy REE (HREE) concentrations. The $\delta^{34}S_{VCDT}$ values vary in a very narrow range from 10.3% to 11.0%, which is much lower than those of the contemporaneous seawater (Claypool et al., 1980). The Rb contents are much lower than the Sr contents, with Rb/Sr ratios of <0.1 (average of 0.014), indicating that the values do not need to be corrected for the decay of Rb to Sr. The $^{87}Sr/^{86}Sr$ ratios of the gypsum samples range from 0.709942 to 0.710062, which are higher than modern seawater (0.70920) and Eocene seawater (0.70755) (McArthur et al., 2012).

Palynological Records and CA Results

Of the 16 samples analyzed, palynomorphs were identified in 10 samples, and the recovery was poor in all of the samples. There are rare palynomorphs in the upper part of the Youzha section, which is likely related to the aridity inferred from the presence of gypsum and halite. Vegetation is usually sparse and their palynomorphs are easily destroyed in arid environments (Yuan et al., 2020). We identified 56 palynomorphs, including 13 spores and 43 pollen taxa (4 gymnosperm and 39 angiosperm morphospecies) (**Figure 5**). The palynoflora are predominantly angiosperm pollen (20.5–95.3%), which are dominant by *Celtispollenites* and *Caryapollenites*, as well as *Tricolpites*, *Tricolporopollenites*, and *Lonicerapollis* (**Figure 6**). Pollen of *Liquidambarpollenites*, *Ulmipollenites*, *Ulmoideipites*, *Juglanspollenites*, *Multiporopollenites*, and *Subtriporopollenites* occur frequently. There are minor amounts of *Pterocaryapollenites*, *Faguspollenites*, *Quercoidites*, *Retitricolpites*, *Aceripollenites*,

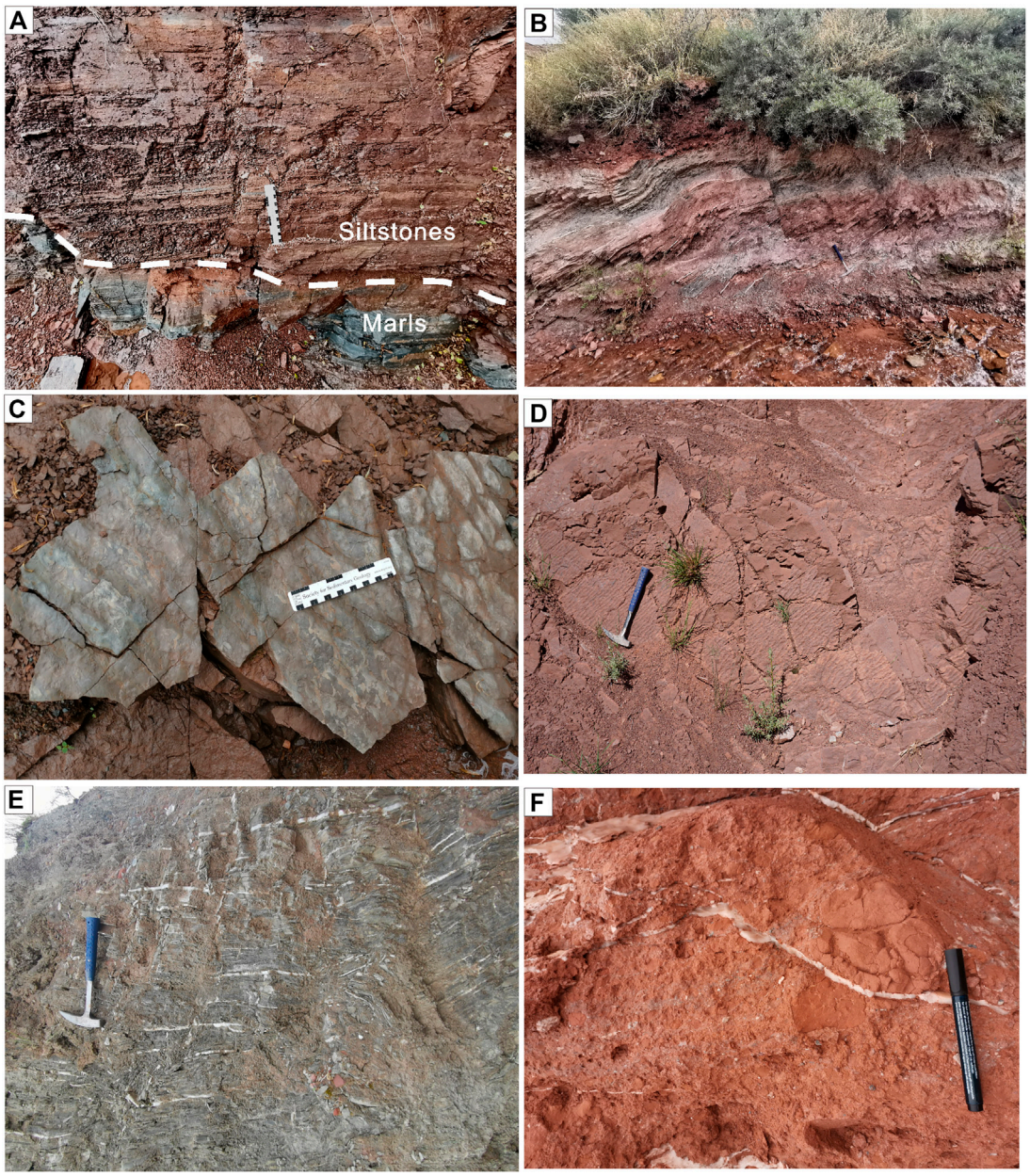

FIGURE 4 | Field photos of the upper part of the Ranmugou Formation, Gonjo Basin. **(A)** The contact between the marls and siltstones in the lower part of section. **(B)** Outcropped photos show the thin-bedded siltstones and marls interbedded with gypsum rocks. **(C,D)** Ripple marks. **(E)** Marls interbedded with gypsum rocks in the upper part of section. **(F)** Conglomerates that are composed of clay gravels show the rock salt solution. Noted that the secondary gypsum veins cut into the conglomerates.

Ranunculacidites, and *Sapotaceoidaepollenites*. The gymnosperm pollen (2.2–9.5%) are mainly from *Ephedripites* and *Taxodiaceaepollenites* with minor *Cycadopites* and *Cedripites*. The ferns include 13 sporomorphs; and the dominant taxa are *Lycopodiumsporites* and *Osmundacidites*; while *Triporoletes, Toroisporites, Pterisporites,* and *Zlivisporis* sporadically appear.

Middle Eocene fossil sporomorphs from the Gonjo Basin were used to reconstruct the MAT and MAP using CA. The estimated paleoclimatic parameters are shown in **Figure 7**. The CA quantitative estimates show a warm and humid climate with a MAT ranging from 13 to 15°C and a MAP of ~1,400 mm.

DISCUSSION

Age Constraints

As was previously stated, the ages of the lacustrine marlstone, mudstone, and evaporite of the upper Ranmugou Formation in

TABLE 1 | The trace and rare Earth element concentrations and sulfur, strontium isotopic composition of gypsum samples from Youzha section, Gonjo Basin.

Sample	GJ-62	GJ-65	GJ-67	GJ-69	Sample	GJ-62	GJ-65	GJ-67	GJ-69
Lithology	Gypsum	Gypsum	Gypsum	Gypsum	Lithology	Gypsum	Gypsum	Gypsum	Gypsum
Li	1.18	0.39	0.756	0.409	La	0.118	0.168	0.301	0.178
Be	0.054	0.063	0.058	0.044	Ce	0.104	0.138	0.225	0.086
Sc	5.5	7.35	5.15	5.01	Pr	0.02	0.028	0.056	0.032
V	35.3	14.8	8.43	7.9	Nd	0.076	0.066	0.168	0.143
Cr	2.09	1	1.21	0.921	Sm	0.016	0.009	0.023	0.027
Co	10.1	10.6	10.9	10.3	Gd	0.018	0.022	0.032	0.025
Ni	15.6	17.4	18.1	17.4	Dy	0.005	0.013	0.011	0.003
Cu	1.47	0.966	1.1	0.923	Er	0.002	0.004	0.002	0.005
Zn	2.08	1.92	2.06	2.6	Yb	<0.002	0.003	<0.002	<0.002
Ga	0.355	0.116	0.184	0.12	Lu	<0.002	0.002	<0.002	0.002
Rb	2.59	0.739	1.65	0.847	Pb	1.02	0.163	0.824	0.333
Sr	104	106	111	95.9	Th	0.025	0.015	0.016	0.008
Y	0.03	0.026	0.02	0.014	U	0.059	0.012	0.035	0.023
Mo	<0.002	0.105	0.044	0.021	Zr	0.841	0.674	0.821	0.469
Cd	0.035	0.016	0.022	0.006	$\delta^{34}S_{VCDT}$/‰	11.0	10.3	10.3	10.5
In	0.01	0.012	0.007	0.012	$^{87}Sr/^{86}Sr$	0.70997 (±22)	0.709942 (±16)	0.710057 (±19)	0.710062 (±21)

TABLE 2 | List of nearest living relatives and the fossil taxa grouped according to the information from the biome studies.

Fossil taxa	Nearest living relatives (NLR)
Cedripites	Cedrus
Taxodiaceaepollenites	Taxodium
Ephedripites	Ephedra
Celtispollenites	Celtis
Caryapollenites	Carya
Liquidambarpollenites	Liquidambar
Betulaceoipollenites	Betulaceae
Ulmipollenites	Ulmus
Juglanspollenites	Juglandaceae
Alnipollenites	Alnus
Ostryoipollenites	Ostrya
Carpinipites	Carpinus
Tiliaepollenites	Tiliaceae
Proteacidites	Proteaceae
Myricipites	Myrica
Salixpollenites	Salix
Aceripollenites	Aceraceae
Lonicerapollis	Lonicera
Araliaceoipollenites	Araliaceae
Quercoidites	Quercus
Faguspollenites	Fagaceae
Ranunculacidites	Ranunculus
Lycopodiumsporites	Lycopodiaceae
Osmundacidites	Osmunda
Lygodiumsporites	Lygodium
Pterisporites	Pteris

the Gonjo Basin are still controversial, especially regarding the differences between the fossil and magnetostratigraphic ages. Sparse sporomorphs fossils indicate a wide age range of Paleocene to Oligocene (BGMRT, 1993; Studnicki-Gizbert et al., 2008). The magnetostratigraphy and volcanic U-Pb studies limited the age from 50 to 40 Ma (Xiong et al., 2020) or from 43.4 to 41.5 Ma (Li et al., 2020) or from 54 to 50 Ma (Xiao et al., 2021) for the upper Ranmugou Formation. The palynoflora assemblages in the Youzha section discussed below give an age of middle Eocene, which is congruent with the isotopic ages in the Qudeng section (Xiong et al., 2020).

The absence of the diagnostic Cretaceous taxa *Cicatricosisporites*, *Schizaeoisporites*, and *Classopollis* (Li et al., 2019a), the predominance of the Paleogene pollen taxa, and the presence of Cretaceous relic taxa *Aequitriradites* (Tripathi, 2008) indicate that the samples from the Youzha section could be early Paleogene in age. The amount of Pinaceae pollen suddenly increased at ~36 Ma in the Xining Basin (Hoorn et al., 2012; Page et al., 2019), which was common during the E/O transition, which predominantly occurred in the Oligocene (Zhang, 1995; Page et al., 2019), indicating that the Youzha section cannot be younger than the latest Eocene. In northwestern China, the Paleocene taxa *Normapolles* and *Proteacidites* are dominant (Song, 1999), but these taxa are absent in our samples, indicating that the sedimentary age of the Youzha section is likely younger than the Paleocene. The assemblage of *Ephedripites*, *Nitrariadites/Nitraripollis*, and *Chenopodipollis* are dominant in the late Eocene Tibetan basins, such as Xining Basin (Hoorn et al., 2012), Jiuquan Basin (Miao et al., 2008), Hoh Xil Basin (Miao et al., 2016), and Nangqian Basin (Yuan et al., 2017; Yuan et al., 2020). Zhang (1995) comprehensively reviewed the Paleogene palynological flora in China and concluded that the xerophytic pollen of Zygophyllaceae flourished in the late Eocene. Tong et al. (2001) reported that the average percentage of *Ephedripites* is 30, 20, and 15% in the halite, glauberite, and purple mudstones, respectively, of the middle and late Eocene evaporites in the Jianghan Basin. Therefore, the lower abundances of *Ephedripites* and *Nitrariadites/Nitraripollis* and the absence of Zygophyllaceae and Chenopodiaceae (Dupont-Nivet et al., 2008) preclude a late Eocene age for the Youzha section. Ulmaceaelate, Betulaceae, and Juglandaceae pollen are significant in the early Eocene strata in southern China (Zhang, 1995). This assemblage is similar to those in the Linzhou Basin, central Tibet (Li et al., 2019a), but it differs from the Eocene Hengyang Basin, where a high percentage of *Ephedripites*

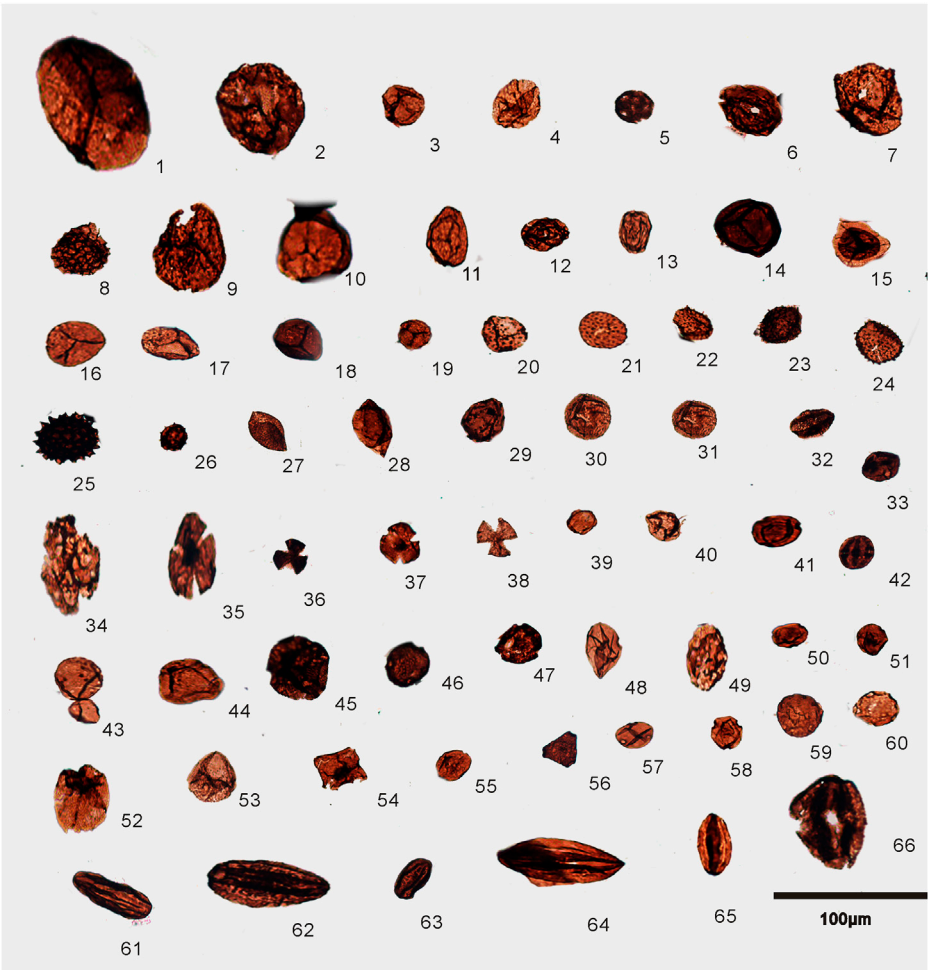

FIGURE 5 | Selected pollen grains and spores from Youzha section, Gonjo Basin. 1: *Hymenophyllumsporites*; 2: *Osmundacidites*; 3: *Triporoletes*; 4: *Leiosphaeridia*; 5: *Liquidambarpollenites*; 6-8: Algae; 9: *Hymenophyllumsporites*; 10: *Triporoletes*; 11: *Osmundacidites*; 12-13: Algae; 14: *Triporoletes*; 15: *Aequitriradites*; 16-21: *Osmundacidites*; 22, 24: *Clavatosporis*; 23: *Echinatisporis*; 25: *Pediastrum*; 26: *Tubulifloridites*; 27: *Liliacidites*; 28: *Magnolipollis*; 29: *Casuarinaepollenites*; 30-31: *Ulmipollenites*; 32: *Salixpollenites*; 33,42: *Sapotaceoidaepollenites*; 34: *Tricolpites*; 35,37. *Ranunculacidites*; 36,38: *Aceripollenites*; 39,40: *Alnipollenites*; 41,48,50: *Myricipites*; 43: *Ptericaryapollenites*. 44: *Ulmoideipites*; 45,46: *Tiliaepollenites*; 47: *Lonicerapollis*; 49: unidentified; 50,51: *Ostryoipollenites*; *52: Leiosphaeridia*; 53: *Lonicerapollis*; 54: unidentified; 55: *Ostryoipollenites*; 56: *Proteacidites*; 57: *Caryapollenites*; 58: *Myricipites*; 59: *Ptericaryapollenites*; 60: *Ptericaryapollenites*; 61-65: *Ephedripites*; 66: *Euphorbiacites.*

was recovered (Xie et al., 2020). The middle Eocene was characterized by dominant tricolporate pollen of Fagaceae and a remarkable decline in triporate to multiporate pollen of the early Eocene taxa (Song and Liu, 1982; Zhang, 1995), although *Ulmipollenites* still account for a large proportion in southern China (Xie et al., 2019). Therefore, the fossil pollen assemblage of *Celtispollenites-Caryapollenites-Tricolpites-Tricolporopollenites* in our samples is similar to the middle Eocene palynoflora records in China. Xiong et al. (2020) gave the age range between 44 Ma and 40 Ma of the lacustrine carbonates from the Ranmugou Formation in the Qudeng section with a thickness of more than 400 m, which is close to the Youzha section. Due to the Quaternary cover, absence of thick salt-solution conglomerates of the upper part of the studied section, and the warm temperate pollen (discussed below) which is inconsistent with the significant cooling since 44 Ma (Xiong et al., 2020), we thus speculate that the age of the section is from 47.8 Ma to >44 Ma.

Paleoenvironmental Reconstruction in the Gonjo Basin

The $\delta^{34}S$ values in our gypsum samples are lower than those of the contemporaneous seawater, which is probably the result of either the reservoir effect (Holser and Kaplan, 1966) or dissolved sulfates with lower $\delta^{34}S$ values in continental water. However, the reservoir effect would not cause lower values in gypsum due to the negligible depletion of ^{34}S in sulfate during gypsum precipitation (Shen et al., 2021). The high $^{87}Sr/^{86}Sr$ values were likely caused by radiogenic ^{87}Sr based on the high Rb/Sr ratios and/or continental

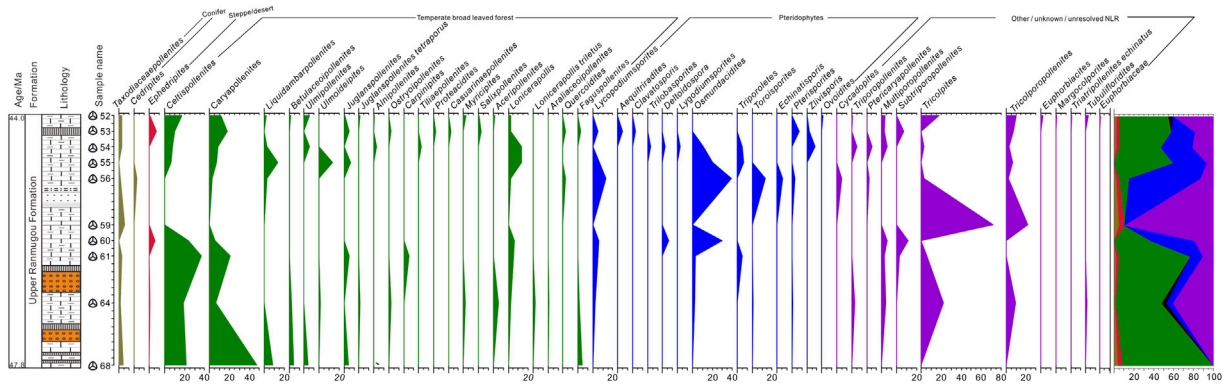

FIGURE 6 | Cumulative pollen summary diagram of the Youzha section in the Gonjo Basin, with palynomorph percentages of the total pollen sum plotted on the *x*-axis.

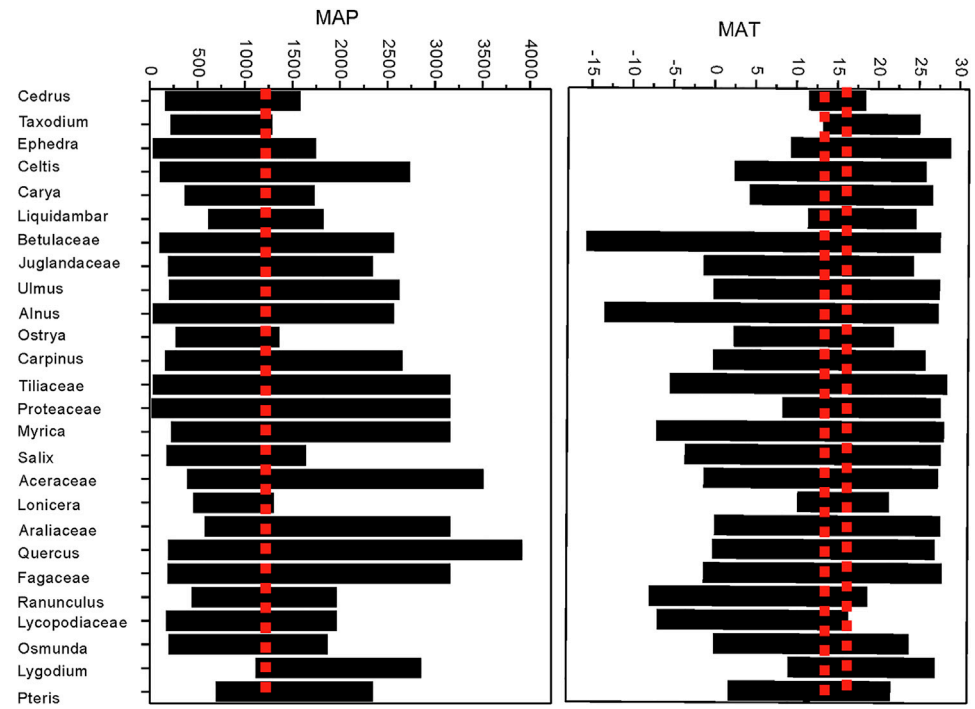

FIGURE 7 | The climatic parameters of MAP and MAT calculated using CA in the Gonjo Basin.

water. Based on the low Rb/Sr ratios, we speculate that continental water was the only reason for the observed high $^{87}Sr/^{86}Sr$ ratios of the gypsum samples. Therefore, we argue that the gypsum was precipitated from a continental water body, not from marine water. The $\delta^{13}C$ and $\delta^{18}O$ values of the marls in the upper part of the Ranmugou Formation have been reported to range from −5.9% to −7.2% and from −16.6% to −13.8%, respectively (Xiong et al., 2020). These values coincide with typical lacustrine carbonates (Talbot, 1990). Thus, during the middle Eocene, the Gonjo Basin was a typical lacustrine environment with input from a continental water body and deep fluids.

The sedimentary sequences in the Youzha section represent a typical lacustrine environment and are characterized by a cycle from saline water to freshwater to hypersaline water (**Figure 3B**). During the saline water stage, lacustrine carbonates and gypsum rocks were deposited, indicating a sulfate deposition stage. In the freshwater stage, fine-grained clastic rocks such as siltstones, mudstones and shales were deposited, indicating that the lake was dilute by influent water. During the hypersaline stage, large amounts of gypsum and halite were deposited when the saline water evaporated and minerals precipitated under hyper-arid conditions. However, due to the unexposed thick halite

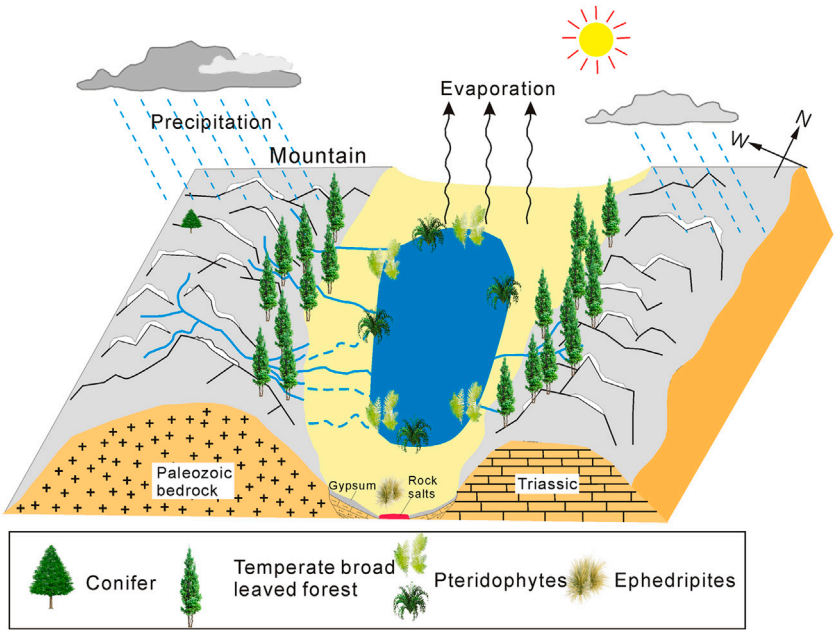

FIGURE 8 | Paleoenvironmental reconstruction in the Gonjo Basin during the interval of 47.8 to >44 Ma (Modified from Yuan et al., 2021), showing the vegetation of broad-leaved trees on slopes and ferns closer to the lake. Very few conifers grew due to the relatively low elevation of the Central Watershed Mountain.

sequences (**Figure 3B**), the hypersalinity in the studied section was not reached.

Our palynological results show that the flora consisted of arbors *Celtispollenites*, Carya, Betulaceae, *Pterocarya*, and *Liquidambar*, and the herbs Caprifoliaceae, Ranunculaceae, Asteraceae, accompanied by the ferns Lycopodiatae and Osmunda, which indicates that the vegetation was a temperate deciduous broad-leaved forest. The abundance of *Celtispollenites* and *Caryapollenites* together with Ulmus, *Taxodiaceaepollenites,* and Juglans suggest a humid and warm climate (e.g., Sun and Wang, 2005; Lu et al., 2020), which is consistent with the CA results. It should be noted that some freshwater algae such as *Pediastrum*, *Leiosphaeridia*, and *Psiloschizosporites* occurred in large amounts in the lower part of the Youzha section, indicating that the depositional environment was near a water body, which is supported by our sedimentary results. In the Youzha section, the xerophytic taxa *Ephedripites* is only found in the lower part (samples GJ-52 and GJ-53) and top part (sample GJ-64) of the section in low abundance. In addition, *Nitrariadites* is absent throughout the section. The Xerophytic shrub *Ephedra* (*Ephedripites*) usually grows in arid environments (Dupont-Nivet et al., 2008). The modern equivalent of *Nitrariadites* is *Nitraria*, which is a steppe-desert taxon (Sun and Wang, 2005). The xerophytic taxa *Ephedripites*, *Nitrariadites*, and Chenopodiaceae are typical in alluvial gravelly plains and treeless alpine desert landscapes with an annual rainfall of <100 mm (Herzschuh et al., 2003; Sun and Wang, 2005). Thus, the paleoenvironment recorded by the pollen assemblages in the Youzha section (47.8–>44 Ma) was a warm and humid temperate deciduous broad-leaved forest (**Figure 8**).

The carbonate clumped isotope thermometry indicates a warm climate, with a temperature of about 24°C, during the early Eocene (54–50 Ma) and a dramatic decrease in temperature to about 7°C during 44–40 Ma (Xiong et al., 2020). Thus, based on our sedimentary and pollen evidence and the isotope-based temperature, we conclude that the paleoenvironment in the Gonjo Basin changed from the warm and humid deciduous broad-leaved forest in the early middle Eocene (47.8–>44 Ma), to the cool and arid temperate forest during 44–40 Ma.

Comparison With Other Middle Eocene Paleovegetation in Western China

Our palynological assemblages are comparable with those in the Kuqa and Yarkand basins (Wang et al., 1986). Our findings indicate a paleoenvironmental change from warm and humid to cool and arid at ~44–40 Ma, which is quite consistent with the change in the Qaidam Basin. The palynological assemblage of the Luluhe Formation (50–43 Ma) in the Qaidam Basin is predominantly *Betulaepollenites-Taxodiaceaepollenites-Potamogetonacidites-Tsugaepollenites*, indicating a deciduous broad-leaved forest and a warm and humid climate (Lu et al., 2020). During 43–41 Ma, a certain amount of the coniferous taxa *Piceaepollenites*, *Pinuspollenites*, and *Abiespollenites* began to appear, suggesting that the climate changed to arid and cool (Lu et al., 2020). These environmental and ecosystem variations are supported by a recent paleoclimate estimate. A quantitative reconstruction suggests that the MAP in the Qaidam Basin was ~800–1,400 mm during ~49–43 Ma, and the MAP and mean temperature of the coldest month (MTCO) declined after ~43 Ma, indicating a climatic change from warm and humid

to cool and arid at ~43 Ma (Jia et al., 2021). The paleoenvironmental variation in the middle Eocene is also regionally corroborated by the records in the Xining Basin. The palynological composition in the Xining Basin changed from abundant *Ulmipollenites* to 80% desert-steppe vegetation at ~40 Ma, indicating significant aridification (Bosboom et al., 2014). The palynofloras are different from those in the Lunpola Basin which is dominated by *Quercoidites-Ulmipollenites-Taxodium* assemblage (Li et al., 2019a). The middle Eocene vegetation in southern China was a mixture of evergreen and deciduous broad-leaved forests, indicating a warm and humid subtropical climate under the influence of the East Asian Monsoon (Xie et al., 2019), which changed from the early Eocene arid desert (Xie et al., 2020).

Paleoenvironmental Evolution and Driving Factors During the Eocene on the Eastern TP

The Eocene sedimentary records in the Xining, Jiuquan, Qaidam, Hoh Xil, and Nangqian basins, which have accurate age control, and their pollen and other climate proxies can provide good climatic and ecological correlations. Large amounts of xerophytic taxa are a significant feature of the late Eocene sedimentary basins in the northeastern TP, such as the Xining (Dupont-Nivet et al., 2008; Hoorn et al., 2012), Jiuquan (Miao et al., 2008), Qaidam (Lu et al., 2020), Hoh Xil (Miao et al., 2016), and Nangqian basins (Yuan et al., 2020). After the MECO (~40 Ma), the Xining Basin was characterized by halophytic and xerophytic vegetation, including *Ephedripites* and *Nitrariadites/Nitraripollis* (Hoorn et al., 2012; Bosboom et al., 2014), with a sudden increase in the high-altitude pollen of Pinaceae at ~37 Ma (Abels et al., 2011; Hoorn et al., 2012). During ~40–33 Ma, arid-semiarid shrubs, represented by *Nitrariadites* and *Chenopodipollis,* prevailed in the Jiuquan Basin (Miao et al., 2008). It should be noted that Pinaceae accounted for 5–25.6% (*Pinuspollenites*, *Abietineaepollenites*, *Piceaepollenites*, and *Abiespollenites*) at ~40 Ma (Miao et al., 2008). This sharp increase in Pinaceae (6.3–32%, *Piceaepollenites*, *Pinuspollenites*, and *Abiespollenites*) also began at 43 Ma in the Qaidam Basin (Lu et al., 2020). The pollen in the late Eocene to Oligocene Yaxicuo Group in the Hoh Xil Basin (Jin et al., 2018; Lin et al., 2020) are predominantly from xerophytic *Ephedripites*, *Nitrariadites,* and *Chenopodipollis* with a low abundance of *Picea* due to the aridity and low elevation in this area (Miao et al., 2016). Thus, the flora in the late Eocene Hoh Xil Basin reflects a subtropical arid climate and the paleoenvironment changed from warm and humid to arid and cool at ~41 Ma (Li et al., 2019a). This is consistent with the cooling trends inferred from clumped isotopes in the Nangqian Basin (Li et al., 2019b). Therefore, the paleoclimate in the northeastern TP basins became to be arid and relatively cool during ~43–40 Ma. It should be noted that the cooling was a long-term and stepwise trend, and it ultimately lead to significant cooling during the Eocene-Oligocene transition (EOT).

The flora in the Markam Basin were previously thought to be Miocene and are currently dated as latest Eocene to earliest Oligocene, reflecting a change from late Eocene subtropical/warm temperate evergreen and deciduous mixed vegetation (mainly represented by Fagaceae and Betulaceae) to early Oligocene cool temperate vegetation (represented by Eosaceae and Salicaceae) (Su et al., 2019; Chen et al., 2021). In the Jianchuan Basin, southwestern Yunnan, the late Eocene flora in the Shuanghe Formation (Gourbet et al., 2017) are characterized by *Caryapollenites*, *Cupuliferoipollenites*, *Alnipollenites*, *Juglanspollenites*, *Pterocaryapollenites*, and *Meliaceoidites*, indicating a temperate deciduous broad-leaved forest (Wu et al., 2018).

As such, based on the flora and climatic records in the TP, it is clear that a warm and humid temperate broad-leaved forest dominated in the northeastern (NE) TP during the middle Eocene (e.g., Gonjo Basin). During ~44–40 Ma, region-wide aridification and cooling prevailed, with significant amounts of conifers and xerophytic shrubs, indicating a cool and arid steppe-desert environment (e.g., Nangqian Basin). During the EOT, which is represented by the flora in the Markam Basin, vegetation indicative of a cool temperate environment dominated. We infer that the paleoenvironmental changes in the Gonjo, Nangqian, and Markam Basins during the middle to late Eocene were forced by the uplift of the Central Watershed Mountain, although several drivers such as global cooling, the retreat of the Paratethys Sea, and the uplift of the TP have been proposed to explain the aridification and cooling on the NE TP (Dupont-Nivet et al., 2008; Bosboom et al., 2014; Zhang et al., 2018; Yuan et al., 2020). The uplift of the Tanggula Shan, Nangqian, Gonjo, and Markam Basins in the Central Watershed Mountain during the middle to late Eocene attained near present elevations. The Tanggula Shan was elevated to about 4,000 m at ~40 Ma based on thermochronologic and structural evidence (Wang et al., 2008). The paleoelevation recovered from *n*-alkane δ^2H data for the Yaxicuo Group indicate that the source of the Tanggula Shan was located at about 4,000 m in the late Eocene (Lin et al., 2020). Carbonate stable and clumped isotopic evidence suggests an altitude of ~3,000 m in the Nangqian Basin and its surrounding mountains during the late Eocene (Li et al., 2019b). Also, the Gonjo Basin reached its elevation of 3,800 m in the 44–40 Ma based on carbonate clumped isotopes (Xiong et al., 2020), while the Markam Basin reached an elevation of about 3,000 m in the latest Eocene (~34 Ma) (Su et al., 2019), indicating the southward expansion of the Central Watershed Mountains. Collectively, the high topography of the Central Watershed Mountain leads to the development and intensification of the Asian monsoon during the middle Eocene (~44–40 Ma) (Xiong et al., 2020; Fang et al., 2021) by blocking the southerly source of moisture and altering the atmospheric circulation (Raymo and Ruddiman, 1992), which is similar to the scenario in the Gangdese Mountains (Ding et al., 2014). The development of the Eocene Asian monsoon was controlled by the paleogeography resulting from the uplift of the TP rather than by the CO_2 concentration (Farnsworth et al., 2019). Recent climate model simulations also suggest that the northward migration of the high-elevation proto-TP intensified the aridity and affected the precipitation (Zhu et al., 2019). As such, we infer that the climate and ecosystem transition since the middle Eocene in the regional-wide Central Watershed Mountain

were largely controlled by the tectonic uplift of the TP rather than by global cooling and the retreat of the Paratethys Sea.

However, for the interior basins in the northern TP, we conclude that global cooling, the uplift of the northern TP, and the retreat of the Paratethys Sea were the combined driving force. First, the rapid decreases in temperature and precipitation in the Qaidam Basin at ~43 Ma were inferred to be caused by global cooling alone (Jia et al., 2021). Similarly, the appearance of high-elevation conifers predated the significant cooling in the EOT in the Xining Basin (Dupont-Nivet et al., 2008), which supports the hypothesis that the stepwise global cooling could not sufficiently drive the paleoenvironmental changes. Second, the increased amount of coniferous taxa reflect the uplift of the surrounding mountains with plant zonation, but the fossils and isotope-based paleoaltimetry indicate relatively low elevations for the interior basins during the middle Eocene (Miao et al., 2008, 2016; Lin et al., 2020). Although model simulations have shown the important role of the uplift of the central TP in the long-term trend of aridification (Li et al., 2018), the short-term fluctuations between dry and wet (Fang et al., 2015; Meijer et al., 2019) cannot be explained by the slow tectonic uplift. Third, the major retreat of the Paratethys Sea from the Tarim Basin at ~41 Ma (Bosboom et al., 2013) was broadly coeval with the stepwise aridification and cooling in the Xining, Jiuquan, Qaidam, and Hoh Xil basins. Moreover, owing to the sustained blocking of the southerly source moisture by the Central Watershed Mountain, the moisture carried by the westerlies was significant to the climate change in these basins. Thus, the retreat was an important driving factor.

CONCLUSION

In this study, we analyzed the palynological assemblages, sedimentary records, and geochemistry of evaporites from the Youzha section in the Gonjo Basin. The conclusions that follow were drawn.

(1) The outcropped section in the Youzha is middle Eocene in age, with an upper age limit of 44 Ma.
(2) This section is indicative of a temperate deciduous broad-leaved forest and a warm and humid climate. The paleoenvironment in the Gonjo Basin changed from the warm and humid forest to the cool and arid forest in 44–40 Ma.
(3) We infer that the regional scale uplift of the Central Watershed Mountain since the middle Eocene largely controlled the climate and ecosystem transitions in the Gonjo, Nangqian, and Markam Basins.

DATA AVAILABILITY STATEMENT

The original contributions presented in the study are included in the article/Supplementary Material, further inquiries can be directed to the corresponding authors.

AUTHOR CONTRIBUTIONS

LW: investigation, writing, review, and revision. QY: writing, review, revision. LS: investigation and review. LD: conceptualization, supervision, and funding acquisition. All authors have read and agreed to the published version of the manuscript.

FUNDING

This research was financially supported by the STEP (Grant nos. QZKK20190803, QZKK20190708), and Strategic Priority Research Program of Chinese Academy of Sciences (Grant No. XDA 20070301).

ACKNOWLEDGMENTS

We thank LetPub (www.letpub.com) for its linguistic assistance during the preparation of this manuscript.

REFERENCES

Abels, H. A., Dupont-Nivet, G., Xiao, G., Bosboom, R., and Krijgsman, W. (2011). Step-wise Change of Asian interior Climate Preceding the Eocene-Oligocene Transition (EOT). *Palaeogeogr. Palaeoclimatol. Palaeoecol.* 299 (3-4), 399–412. doi:10.1016/j.palaeo.2010.11.028

BGMRT (1993). *Regional Geology of Xizang (Tibet) Autonomous Region*. Beijing: Geological Publish House. Geological Memoirs Series. (in Chinese with English abstract).

Bohaty, S. M., and Zachos, J. C. (2003). Significant Southern Ocean Warming Event in the Late Middle Eocene. *Geology* 31 (11), 1017–1020. doi:10.1130/G19800.1

Bosboom, R., Dupont-Nivet, G., Grothe, A., Brinkhuis, H., Villa, G., Mandic, O., et al. (2014). Linking Tarim Basin Sea Retreat (West China) and Asian Aridification in the Late Eocene. *Basin Res.* 26 (5), 621–640. doi:10.1111/bre.12054

Bosboom, R. E., Abels, H. A., Hoorn, C., van den Berg, B. C. J., Guo, Z., and Dupont-Nivet, G. (2014). Aridification in continental Asia after the Middle Eocene Climatic Optimum (MECO). *Earth Planet. Sci. Lett.* 389, 34–42. doi:10.1016/j.epsl.2013.12.014

Chen, K. G. (1990). Geological Characteristics of the Youzha Rock Salts Deposits in Tibet. *Tibetan Geology* 1, 87–97.

Chen, L., Deng, W., Su, T., Li, S., and Zhou, Z. (2021). Late Eocene Sclerophyllous Oak from Markam Basin, Tibet, and its Biogeographic Implications. *Sci. China Earth Sci.* 64, 1969–1981. doi:10.1007/s11430-020-9826-4

Claypool, G. E., Holser, W. T., Kaplan, I. R., Sakai, H., and Zak, I. (1980). The Age Curves of Sulfur and Oxygen Isotopes in marine Sulfate and Their Mutual Interpretation. *Chem. Geology* 28, 199–260. doi:10.1016/0009-2541(80)90047-9

Cramwinckel, M. J., Huber, M., Kocken, I. J., Agnini, C., Bijl, P. K., Bohaty, S. M., et al. (2018). Synchronous Tropical and Polar Temperature Evolution in the Eocene. *Nature* 559 (7714), 382–386. doi:10.1038/s41586-018-0272-2

Ding, L., Xu, Q., Yue, Y., Wang, H., Cai, F., and Li, S. (2014). The Andean-type Gangdese Mountains: Paleoelevation Record from the Paleocene-Eocene Linzhou Basin. *Earth Planet. Sci. Lett.* 392, 250–264. doi:10.1016/j.epsl.2014.01.045

Dupont-Nivet, G., Hoorn, C., and Konert, M. (2008). Tibetan Uplift Prior to the Eocene-Oligocene Climate Transition: Evidence from Pollen Analysis of the Xining Basin. *Geology* 36 (12), 987–990. doi:10.1130/G25063A.1

Eldrett, J. S., Greenwood, D. R., Harding, I. C., and Huber, M. (2009). Increased Seasonality through the Eocene to Oligocene Transition in Northern High Latitudes. *Nature* 459 (7249), 969–973. doi:10.1038/nature08069

Fang, X., Yan, M., Zhang, W., Nie, J., Han, W., Wu, F., et al. (2021). Paleogeography Control of Indian Monsoon Intensification and Expansion at 41 Ma. *Sci. Bull.* 66 (22), 2320–2328. doi:10.1016/j.scib.2021.07.023

Fang, X., Zan, J., Appel, E., Lu, Y., Song, C., Dai, S., et al. (2015). An Eocene-Miocene Continuous Rock Magnetic Record from the Sediments in the Xining Basin, NW China: Indication for Cenozoic Persistent Drying Driven by Global Cooling and Tibetan Plateau Uplift. *Geophys. J. Int.* 201 (1), 78–89. doi:10.1093/gji/ggv002

Farnsworth, A., Lunt, D. J., Robinson, S. A., Valdes, P. J., Roberts, W. H. G., Clift, P. D., et al. (2019). Past East Asian Monsoon Evolution Controlled by Paleogeography, Not CO_2. *Sci. Adv.* 5 (10), eaax1697. doi:10.1126/sciadv.aax1697

Gourbet, L., Leloup, P. H., Paquette, J.-L., Sorrel, P., Maheo, G., Wang, G., et al. (2017). Reappraisal of the Jianchuan Cenozoic basin Stratigraphy and its Implications on the SE Tibetan Plateau Evolution. *Tectonophysics* 700-701, 162–179. doi:10.1016/j.tecto.2017.02.007

Grimm, G. W., and Denk, T. (2012). Reliability and Resolution of the Coexistence Approach - A Revalidation Using Modern-Day Data. *Rev. Palaeobotany Palynology* 172, 33–47. doi:10.1016/j.revpalbo.2012.01.006

He, S. Y., Tian, Y. H., Chen, K. G., Chen, Q. Y., and Wen, H. C. (1983). "Paleogene Gonjo Red Beds in East Tibet," in *Contributions to Tibetan Geology*. Editor T. D. Li (Beijing: Geological Publish House), No. 3, 233–242. (in Chinese with English abstract).

Herzschuh, U., Kürschner, H., and Ma, Y. (2003). The Surface Pollen and Relative Pollen Production of the Desert Vegetation of the Alashan Plateau, Western Inner Mongolia. *Sci. Bull.* 48 (14), 1488–1493. doi:10.1360/02wd0256

Holser, W. T., and Kaplan, I. R. (1966). Isotope Geochemistry of Sedimentary Sulfates. *Chem. Geology* 1, 93–135. doi:10.1016/0009-2541(66)90011-8

Hoorn, C., Straathof, J., Abels, H. A., Xu, Y., Utescher, T., and Dupont-Nivet, G. (2012). A Late Eocene Palynological Record of Climate Change and Tibetan Plateau Uplift (Xining Basin, China). *Palaeogeogr. Palaeoclimatol. Palaeoecol.* 344-345, 16–38. doi:10.1016/j.palaeo.2012.05.011

Jia, Y., Wu, H., Zhang, W., Li, Q., Yu, Y., Zhang, C., et al. (2021). Quantitative Cenozoic Climatic Reconstruction and its Implications for Aridification of the Northeastern Tibetan Plateau. *Palaeogeogr. Palaeoclimatol. Palaeoecol.* 567, 110244. doi:10.1016/j.palaeo.2021.110244

Jin, C., Liu, Q., Liang, W., Roberts, A. P., Sun, J., Hu, P., et al. (2018). Magnetostratigraphy of the Fenghuoshan Group in the Hoh Xil Basin and its Tectonic Implications for India-Eurasia Collision and Tibetan Plateau Deformation. *Earth Planet. Sci. Lett.* 486, 41–53. doi:10.1016/j.epsl.2018.01.010

Li, J., Wu, Y., Batten, D. J., and Lin, M. (2019a). Vegetation and Climate of the central and Northern Qinghai-Xizang Plateau from the Middle Jurassic to the End of the Paleogene Inferred from Palynology. *J. Asian Earth Sci.* 175, 35–48. doi:10.1016/j.jseaes.2018.08.012

Li, L., Fan, M., Davila, N., Jesmok, G., Mitsunaga, B., Tripati, A., et al. (2019b). Carbonate Stable and Clumped Isotopic Evidence for Late Eocene Moderate to High Elevation of the East-central Tibetan Plateau and its Geodynamic Implications. *Geol. Soc. Am. Bull.* 131 (5–6), 831–844. doi:10.1130/B32060.1

Li, S., van Hinsbergen, D. J. J., Najman, Y., Liu-Zeng, J., Deng, C., and Zhu, R. (2020). Does Pulsed Tibetan Deformation Correlate with Indian Plate Motion Changes. *Earth Planet. Sci. Lett.* 536, 116144. doi:10.1016/j.epsl.2020.116144

Li, X., Zhang, R., Zhang, Z., and Yan, Q. (2018). What Enhanced the Aridity in Eocene Asian Inland: Global Cooling or Early Tibetan Plateau Uplift. *Palaeogeogr. Palaeoclimatol. Palaeoecol.* 510, 6–14. doi:10.1016/j.palaeo.2017.10.029

Lin, J., Dai, J. G., Zhuang, G., Jia, G., Zhang, L., Ning, Z., et al. (2020). Late Eocene-Oligocene High Relief Paleotopography in the North Central Tibetan Plateau: Insights from Detrital Zircon U-Pb Geochronology and Leaf Wax Hydrogen Isotope Studies. *Tectonics* 39 (2), e2019TC005815. doi:10.1029/2019TC005815

Lu, J. F., Zhang, K. X., Song, B. W., Xu, Y. D., Zhang, J. Y., Huang, W., et al. (2020). Paleogene-Neogene Pollen and Climate Change in Dahonggou Region of Qaidam Basin. *Geoscience* 34 (4), 732–744. (in Chinese with English abstract). doi:10.19657/j.geoscience.1000-8527.2020.027

McArthur, J. M., Howarth, R. J., and Shields, G. A. (2012). "Strontium Isotope Stratigraphy," in *The Geologic Time Scale*. Editor F. M. Gradstein (Amsterdam: Elsevier), 127–144. doi:10.1016/b978-0-444-59425-9.00007-x

Meijer, N., Dupont-Nivet, G., Abels, H. A., Kaya, M. Y., Licht, A., Xiao, M., et al. (2019). Central Asian Moisture Modulated by Proto-Paratethys Sea Incursions since the Early Eocene. *Earth Planet. Sci. Lett.* 510, 73–84. doi:10.1016/j.epsl.2018.12.031

Metcalfe, I. (2013). Gondwana Dispersion and Asian Accretion: Tectonic and Palaeogeographic Evolution of Eastern Tethys. *J. Asian Earth Sci.* 66, 1–33. doi:10.1016/j.jseaes.2012.12.020

Miao, Y., Fang, X., Song, Z., Wu, F., Han, W., Dai, S., et al. (2008). Late Eocene Pollen Records and Palaeoenvironmental Changes in Northern Tibetan Plateau. *Sci. China Earth Sci.* 51 (8), 1089–1098. doi:10.1007/s11430-008-0091-7

Miao, Y., Wu, F., Chang, H., Fang, X., Deng, T., Sun, J., et al. (2016). A Late-Eocene Palynological Record from the Hoh Xil Basin, Northern Tibetan Plateau, and its Implications for Stratigraphic Age, Paleoclimate and Paleoelevation. *Gondwana Res.* 31, 241–252. doi:10.1016/j.gr.2015.01.007

Mosbrugger, V., and Utescher, T. (1997). The Coexistence Approach-A Method for Quantitative Reconstruction of Tertiary Terrestrial Palaeoclimate Data Using Plant Fossils. *Palaeogeogr. Palaeoclimatol. Palaeoecol.* 134, 61–86. doi:10.1016/S0031-0182(96)00154-X

Page, M., Licht, A., Dupont-Nivet, G., Meijer, N., Barbolini, N., Hoorn, C., et al. (2019). Synchronous Cooling and Decline in Monsoonal Rainfall in Northeastern Tibet during the Fall into the Oligocene Icehouse. *Geology* 47 (3), 203–206. doi:10.1130/G45480.1

Quan, C., Liu, Y.-S., and Utescher, T. (2012). Eocene Monsoon Prevalence over China: a Paleobotanical Perspective. *Palaeogeogr. Palaeoclimatol. Palaeoecol.* 365-366, 302–311. doi:10.1016/j.palaeo.2012.09.035

Raymo, M. E., and Ruddiman, W. F. (1992). Tectonic Forcing of Late Cenozoic Climate. *Nature* 359 (6391), 117–122. doi:10.1038/359117a0

Shen, L., Wang, L., Liu, C., and Zhao, Y. (2021). Sr, S, and O Isotope Compositions of Evaporites in the Lanping-Simao Basin, China. *Minerals* 11 (2), 96. doi:10.3390/min11020096

Song, Z. C. (1999). *Fossil Spores and Pollen of China*, Vol. 1. Beijing: Science Press. The late Cretaceous and Tertiary.

Song, Z. C., and Liu, J. L. (1982). *The Tertiary Sporopollen Assemblages from Namling of Xizang. Palaeonotology of Xiang*. Beijing: Science Press, 153–164. (in Chinese with English abstract).

Studnicki-Gizbert, C., Burchfiel, B. C., Li, Z., and Chen, Z. (2008). Early Tertiary Gonjo basin, Eastern Tibet: Sedimentary and Structural Record of the Early History of India-Asia Collision. *Geosphere* 4 (4), 713–735. doi:10.1130/ges00136.1

Su, T., Spicer, R. A., Li, S.-H., Xu, H., Huang, J., Sherlock, S., et al. (2019). Uplift, Climate and Biotic Changes at the Eocene-Oligocene Transition in South-Eastern Tibet. *Natl. Sci. Rev.* 6 (3), 495–504. doi:10.1093/nsr/nwy062

Sun, X., and Wang, P. (2005). How Old Is the Asian Monsoon System?-Palaeobotanical Records from China. *Palaeogeogr. Palaeoclimatol. Palaeoecol.* 222 (3-4), 181–222. doi:10.1016/j.palaeo.2005.03.005

Talbot, M. R. (1990). A Review of the Palaeohydrological Interpretation of Carbon and Oxygen Isotopic Ratios in Primary Lacustrine Carbonates. *Chem. Geology* 80 (4), 261–279. doi:10.1016/0168-9622(90)90009-2

Tang, H., Li, S.-F., Su, T., Spicer, R. A., Zhang, S.-T., Li, S.-H., et al. (2020). Early Oligocene Vegetation and Climate of Southwestern China Inferred from Palynology. *Palaeogeogr. Palaeoclimatol. Palaeoecol.* 560, 109988. doi:10.1016/j.palaeo.2020.109988

Tang, M., Liu-Zeng, J., Hoke, G. D., Xu, Q., Wang, W., Li, Z., et al. (2017). Paleoelevation Reconstruction of the Paleocene-Eocene Gonjo basin, SE-central Tibet. *Tectonophysics* 712-713, 170–181. doi:10.1016/j.tecto.2017.05.018

Tong, G. B., Zheng, M., Yuan, H., Liu, J., Li, Y., and Wang, W. (2001). A Study of Middle and Late Eocene Palynological Assemblages in Jianghan Basin and Their Environmental Significance. *Acta Geoscientica Sinica* 22, 73–78. (in Chinese with English abstract).

Tong, Y., Yang, Z., Mao, C., Pei, J., Pu, Z., and Xu, Y. (2017). Paleomagnetism of Eocene Red-Beds in the Eastern Part of the Qiangtang Terrane and its Implications for Uplift and Southward Crustal Extrusion in the southeastern Edge of the Tibetan Plateau. *Earth Planet. Sci. Lett.* 475, 1–14. doi:10.1016/j.epsl.2017.07.026

Tripathi, A. (2008). Palynochronology of Lower Cretaceous Volcano-Sedimentary Succession of the Rajmahal Formation in the Rajmahal Basin, India. *Cretaceous Res.* 29 (5-6), 913–924. doi:10.1016/j.cretres.2008.05.008

Utescher, T., Bruch, A. A., Erdei, B., François, L., Ivanov, D., Jacques, F. M. B., Kern, A. K., Liu, Y.-S., Mosbrugger, V., and Spicer, R. A. (2014). The Coexistence Approach-Theoretical Background and Practical Considerations of Using Plant Fossils for Climate Quantification. *Palaeogeogr. Palaeoclimatol. Palaeoecol.* 410, 58–73. doi:10.1016/j.palaeo.2014.05.031

Utescher, T., and Mosbrugger, V. P. (1997). PALAEOFLORA Database. http://www.palaeoflora.de/.

Wang, C., Zhao, X., Liu, Z., Lippert, P. C., Graham, S. A., Coe, R. S., et al. (2008). Constraints on the Early Uplift History of the Tibetan Plateau. *PNAS* 105 (13), 4987–4992. doi:10.1073/pnas.0703595105

Wang, D. N., Sun, X. Y., and Zhao, Y. N. (1986). Palynoflora from Late Cretaceous to Tertiary in Qinghai and Xinjiang. *Bull. Inst. Geol. CAGS*, 15, 152–165. (in Chinese with English abstract).

Wu, J., Zhang, K., Xu, Y., Wang, G., Garzione, C. N., Eiler, J., et al. (2018). Paleoelevations in the Jianchuan Basin of the southeastern Tibetan Plateau Based on Stable Isotope and Pollen Grain Analyses. *Palaeogeogr. Palaeoclimatol. Palaeoecol.* 510, 93–108. doi:10.1016/j.palaeo.2018.03.030

Xia, W. J., and Li, X. H. (1983). About the Theoretic Original Study of Evaporites — from the Potash-Halite deposit in Mengyejing Yunnan. *J. Mineral. Petrol.* 9, 1–11. (in Chinese with English abstract).

Xiao, R., Zheng, Y., Liu, X., Yang, Q., Liu, G., Xia, L., et al. (2021). Synchronous Sedimentation in Gonjo Basin, Southeast Tibet in Response to India-Asia Collision Constrained by Magnetostratigraphy. *Geochem. Geophys. Geosyst* 22 (3), e2020GC009411. doi:10.1029/2020GC009411

Xie, Y., Wu, F., and Fang, X. (2019). Middle Eocene East Asian Monsoon Prevalence over Southern China: Evidence from Palynological Records. *Glob. Planet. Change* 175, 13–26. doi:10.1016/j.gloplacha.2019.01.019

Xie, Y., Wu, F., Fang, X., Zhang, D., and Zhang, W. (2020). Early Eocene Southern China Dominated by Desert: Evidence from a Palynological Record of the Hengyang Basin, Hunan Province. *Glob. Planet. Change* 195, 103320. doi:10.1016/j.gloplacha.2020.103320

Xiong, Z., Ding, L., Spicer, R. A., Farnsworth, A., Wang, X., Valdes, P. J., et al. (2020). The Early Eocene Rise of the Gonjo Basin, SE Tibet: From Low Desert to High forest. *Earth Planet. Sci. Lett.* 543, 116312. doi:10.1016/j.epsl.2020.116312

Yin, A., and Harrison, T. M. (2000). Geologic Evolution of the Himalayan-Tibetan Orogen. *Annu. Rev. Earth Planet. Sci.* 28 (1), 211–280. doi:10.1146/annurev.earth.28.1.211

Yuan, Q., Barbolini, N., Ashworth, L., Rydin, C., Gao, D.-L., Shan, F.-S., et al. (2021). Palaeoenvironmental Changes in Eocene Tibetan lake Systems Traced by Geochemistry, Sedimentology and Palynofacies. *J. Asian Earth Sci.* 214, 104778. doi:10.1016/j.jseaes.2021.104778

Yuan, Q., Barbolini, N., Rydin, C., Gao, D.-L., Wei, H.-C., Fan, Q.-S., et al. (2020). Aridification Signatures from Fossil Pollen Indicate a Drying Climate in East-central Tibet during the Late Eocene. *Clim. Past* 16 (6), 2255–2273. doi:10.5194/cp-16-2255-2020

Yuan, Q., Vajda, V., Li, Q.-K., Fan, Q.-S., Wei, H.-C., Qin, Z.-J., et al. (2017). A Late Eocene Palynological Record from the Nangqian Basin, Tibetan Plateau: Implications for Stratigraphy and Paleoclimate. *Palaeoworld* 26 (2), 369–379. doi:10.1016/j.palwor.2016.10.003

Zachos, J. C., Dickens, G. R., and Zeebe, R. E. (2008). An Early Cenozoic Perspective on Greenhouse Warming and Carbon-Cycle Dynamics. *Nature* 451 (7176), 279–283. doi:10.1038/nature06588

Zachos, J., Pagani, M., Sloan, L., Thomas, E., and Billups, K. (2001). Trends, Rhythms, and Aberrations in Global Climate 65 Ma to Present. *Science* 292 (5517), 686–693. doi:10.1126/science.1059412

Zhai, Q.-G., Zhang, R.-Y., Jahn, B.-M., Li, C., Song, S.-G., and Wang, J. (2011). Triassic Eclogites from central Qiangtang, Northern Tibet, China: Petrology, Geochronology and Metamorphic P-T Path. *Lithos* 125 (1-2), 173–189. doi:10.1016/j.lithos.2011.02.004

Zhang, K., Wang, G., Chen, F., Xu, Y., Luo, M., Xiang, S., et al. (2007). Coupling between the Uplift of the Tibetan Plateau and Distribution of Basins of Paleogene to Neogene. *Earth Sci.* 32 (5), 583–597. (in Chinese with English abstract).

Zhang, R., Jiang, D., Ramstein, G., Zhang, Z., Lippert, P. C., and Yu, E. (2018). Changes in Tibetan Plateau Latitude as an Important Factor for Understanding East Asian Climate since the Eocene: A Modeling Study. *Earth Planet. Sci. Lett.* 484, 295–308. doi:10.1016/j.epsl.2017.12.034

Zhang, Y. Y. (1995). Outline of Palaeogene Palynofloras of China. *Acta Palaeontologica Sinica* 34 (2), 212–227.

Zhu, C., Meng, J., Hu, Y., Wang, C., and Zhang, J. (2019). East-Central Asian Climate Evolved with the Northward Migration of the High Proto-Tibetan Plateau. *Geophys. Res. Lett.* 46 (14), 8397–8406. doi:10.1029/2019GL082703

Conflict of Interest: The authors declare that the research was conducted in the absence of any commercial or financial relationships that could be construed as a potential conflict of interest.